

# A Focal Plane Imager with High Dynamic Range to Identify Fabrication Errors in Diffractive Optics

M. Imran Afzal, Sofia C. Corzo-Garcia, Ulf Griesmann

National Institute of Standards and Technology (NIST), Engineering Physics Division, Gaithersburg, MD 20899-8220, USA  
muhammad.afzal@nist.gov

**Abstract:** We describe the prototype of a focal plane imager for the characterization of fabrication errors in diffractive optics. We also demonstrate the use of a high dynamic range imaging method to identify small errors in a hologram and a grating that can be traced to the fabrication method.  
OCIS codes: (050.0050) Diffraction and gratings; (090.0090) Holography; (120.3930) Metrological instrumentation; (120.3940) Metrology

## 1. Introduction

All micro-fabrication methods used in the fabrication of diffractive optics impart characteristic fabrication errors to the diffractive optic. Especially when diffractive optics are used in demanding imaging applications it is important that those fabrication errors are carefully characterized, well understood, and eliminated. Otherwise fabrication errors result in light being scattered in unwanted directions causing flare and reduced contrast, or even ghost images. The metrology methods most familiar to optics fabricators are not best suited to the evaluation of fabrication errors in diffractive optics. Optical interferometers are only useful for measurements in a small spatial frequency range near zero, and microscope-based inspection systems have a very limited field of view that is typically much smaller than the diffractive surface. Here we describe a prototype measurement system that analyzes the light reflected by a diffraction grating or diffractive optic in the focal (Fourier) plane of a lens, with the goal to separate the small amount of stray light caused by fabrication errors from the strong signal of the light diffracted at the design angle. This idea is not new. A focal plane scanner was used many years ago to evaluate the intensities of ghost lines present in diffraction gratings produced at the Mount Wilson Observatory [1]. A similar focal plane scanner using contemporary technology was described recently for the evaluation of errors in gratings that were fabricated with e-beam lithography [2].

These focal plane scanners have an important limitation. While they can achieve the necessary dynamic range, the measurements are only one-dimensional, the signal at the focal plane of a focusing lens is inherently two-dimensional. The prototype focal plane imager we describe here is designed to overcome this limitation of the focal plane scanners. The light reflected by a grating or the sub-aperture of a diffractive optic is focused on a charge coupled device (CCD) sensor using a lens. An additional innovation is our use of a high dynamic range (HDR) imaging method to achieve the required high dynamic range. We describe the design of the focal plane imager and illustrate its performance – and its current limitations – with measurements of three different gratings.

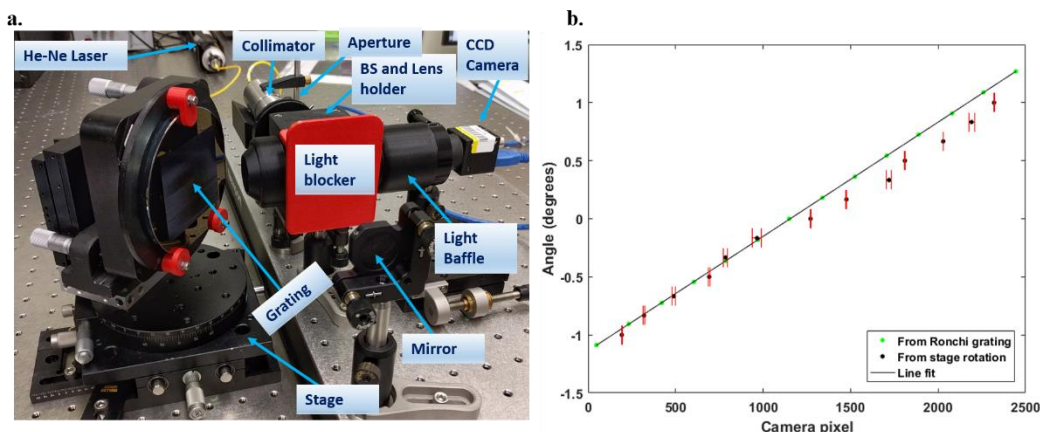


Figure 1. Measurement setup (a) and diffraction angle calibration of the camera (b). The mean of the detector position repeatabilities indicated by the error bars is 7.9 pixels ( $1\sigma$ ). The jump in the stage angle data is due to backlash.

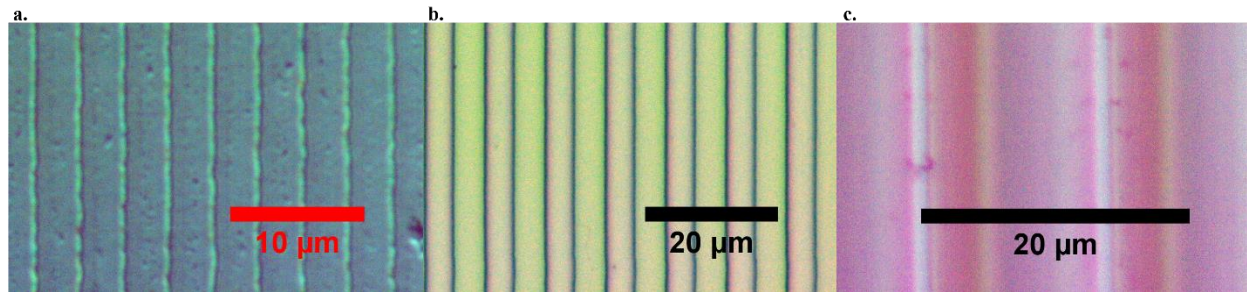


Figure 2. Microscope images of a mechanically ruled blazed grating (a), a binary computer-generated phase hologram (b), and a silicon echelle grating (c).

## 2. Measurement setup

The measurement setup is shown in Fig. 1a. Light from a frequency stabilized helium-neon (He-Ne) laser operating at 632.8 nm is transferred from the laser to a laser collimator by a single mode optical fiber. It is important that the laser collimator produces a well-apodized Gaussian beam that is not diffracted at the collimator. The measurements described here were made with a commercial laser collimator that has an exit aperture of 24 mm diameter and the beam diameter of the Gaussian beam at the  $1/e^2$  point is approximately 11 mm. No diffraction effects due to the collimator (“ringing”) were observed even in the measurements with the highest dynamic range. The collimator is followed by an iris aperture that remained fully open during measurements. The iris is only used to create a narrow beam for alignment purposes. A beam splitter (BS in Fig. 1) reflects 50% of the light from the laser collimator at a right angle onto the grating under test. The test gratings are mounted on a simple manual 5-axis mount that can be seen to the left in Fig. 1a. The main feature of the mount is a rotation stage that is used to rotate the grating until the Littrow condition is met and the test beam is retro-reflected by the grating for the desired diffraction order. Light reflected by the test grating traverses the beam splitter and is focused by a plano-convex lens with 100 mm focal length onto the CCD image detector in the camera. The second beam exiting the beam splitter is blocked by an absorber (attached to the red holder in Fig. 1a) in the measurements described here. We found the design of the beam splitter to be critical for measurements with low stray light level. The measurements described in the following section were made with a cube beam splitter with 25.4 mm edge length. A cube beam splitter is not ideal because the cube faces, even with good anti-reflection (AR) coating, cause substantial stray reflections that reach the camera. A custom beam splitter is being fabricated, but it was not available at the time the measurements described here were made. The camera has an uncooled 2/3 inch CCD sensor with 2448 x 2048 pixels and 12 bits resolution (6.5 bits noise). The window of the camera housing and the cover glass on the image sensor were both removed to eliminate interference and stray light. The camera is mounted on a translation stage to enable us to position it precisely at the focus of the lens. Light baffles reduce the amount of stray light reaching the camera and during measurements the whole setup was enclosed in a box that was made from black foam board and sealed with black caulk.

Both gain and exposure time of the camera can be programmed in a wide range. Images were acquired for 18 settings of gain and exposure time with increasing sensitivity. For each of the settings 10 images were acquired and averaged. Using the gain and exposure time settings the images were scaled onto a common intensity scale and were averaged after removing saturated pixels and the noise floor from each of the 18 images. The result is a single HDR image with a dynamic range of about  $10^7$ . The calibration of the lateral image scale in terms of the (relative) diffraction angle was accomplished in two ways. A mirror was mounted in the test mount and the position of the reflection on the image detector was determined. The mirror was then rotated by small angle increments that could be measured using a Vernier angle scale on the rotation stage and the reflection position was noted for each of the angles. The result is shown in Fig. 1b. The error bars indicate the position repeatability ( $1\sigma$ ) for five repeat measurements. The angle scale was also calibrated using a chrome-on-glass Ronchi grating with a period of 100  $\mu\text{m}$ , which creates 14 diffraction peaks across the image detector. The known angular separation of the peaks is then used to establish the angle scale and the result is also shown in Fig. 1b.

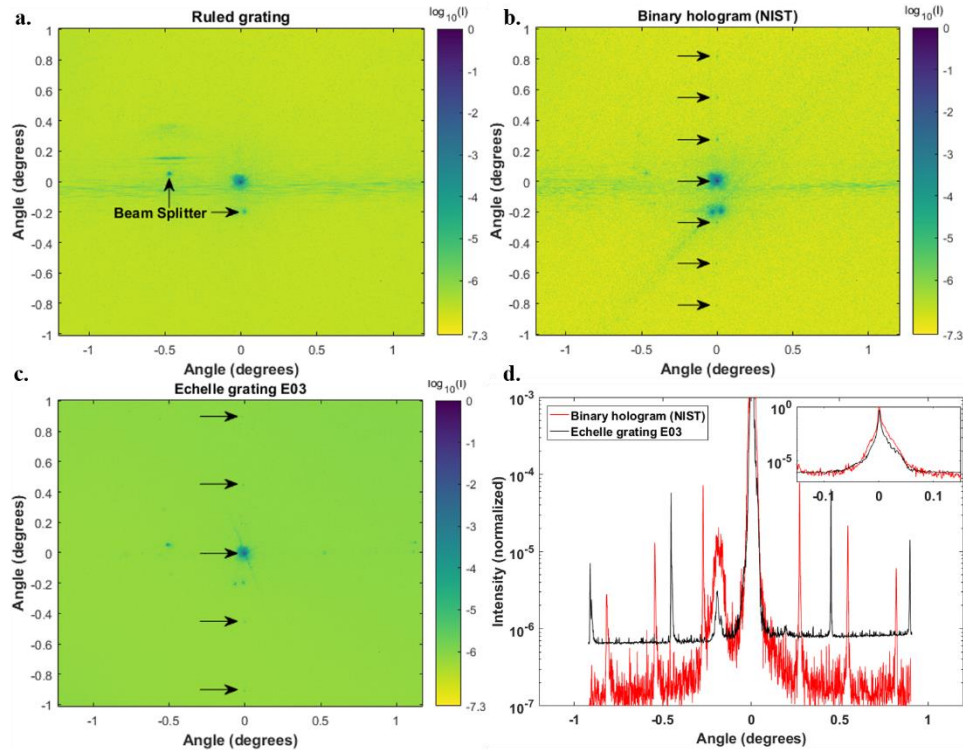


Figure 3. Focal plane images for the 1<sup>st</sup> diffraction order of the mechanically ruled grating (a), the 1<sup>st</sup> diffraction order of the binary phase hologram (b), the 26<sup>th</sup> diffraction order of the echelle grating (c), and sections in the direction of the ordinate through the peak intensity in images b, and c (see graph d). In all images the peak intensity is normalized to one.

### 3. Measurements and Discussion

Three different gratings were investigated with the focal plane imager. Micrographs of the gratings are shown in Fig. 2. The first is a commercial ruled grating with a dimension of 25.4 mm x 25.4 mm and 11° blaze angle (Fig. 2a). The second grating, strictly speaking, not a linear grating but a computer-generated binary phase hologram etched into borosilicate glass, that was made at NIST for measuring the form errors of an elliptic x-ray mirror [3] (Fig. 2b). The hologram has nearly straight zones. The third grating is an immersed silicon echelle grating that was fabricated at the University of Texas at Austin [4]. While the grating is designed to be used in the infrared through the silicon substrate, we used it as a first surface grating at 37° angle of incidence (26<sup>th</sup> order) in our measurement.

Fig. 3 shows the focal plane HDR images that were obtained for the three gratings with the procedure described in section 2. Several strong reflections from the beam splitter cube faces are visible in all focal plane images in Fig. 3. Images 3a and 3b have a horizontal streak of stray light across the image that could be traced to light from non-axial diffraction orders that was scattered by the mount for the beam splitter and the focusing lens. The most intriguing observation are the small, vertically distributed peaks in Figs. 3b and 3c (arrows). In case of Fig. 3b, we can trace them to an error in the hologram with  $(66.4 \pm 0.1)$  μm period that is caused by the step-and-scan motion of the lithography system that was used to create the hologram. This error was not discernible in interferometric measurements. Fig. 3c suggests that a similar periodic fabrication error is present in the silicon echelle grating.

### 4. Acknowledgments

We are grateful to Dr. Cynthia Brooks and Ben Kidder of the University of Texas at Austin for the loan of a silicon echelle grating. The phase grating in Fig. 2b was fabricated using resources provided by the Center for Nanoscale Science and Technology (CNST) NanoFab at NIST. Supported in part by NASA APRA grant NNH15AB22I.

### 5. References

- [1] H. B. Babcock and H. W. Babcock, "The ruling of diffraction gratings at the Mount Wilson Observatory", *JOSA* **41**, 776-786 (1951).
- [2] M. Heusinger, M. Banasch, T. Flügel-Paul, and U.-D. Zeitner, "Investigation and optimization of Rowland ghosts in high efficiency spectrometer gratings fabricated by e-beam lithography", *Proc. SPIE* 9759, 97590A (2016).
- [3] Q. Wang, U. Griesmann, J. Soons, and L. Assoufid, "Figure metrology for x-ray focusing mirrors with Fresnel holograms and photon sieves", *Optical Fabrication & Testing, Kona, Hawaii 2014*, OSA Technical Digest (online) paper OTU4A.5.
- [4] C. B. Brooks, B. Kidder, M. Grigas, U. Griesmann, D. W. Wilson, R. E. Muller, D. T. Jaffe, "Process improvements in the production of silicon immersion gratings," *Proc. SPIE* 9912, 99123Z (2016).